

# A Deep Neural Network Solution For Malignant Melanoma Detection

**Bishwa Raj Poudel, Bibash Adhikari, Amrit Koirala, Sunil Dahal**

Tribhuvan University, Institute of Engineering, Pashchimanchal Campus,  
Department of Electronics and Computer Engineering, Lamachour – 16, Pokhara, Nepal  
*71bct617.bishwa@wrc.edu.np*

Tribhuvan University, Institute of Engineering, Pashchimanchal Campus,  
Department of Electronics and Computer Engineering, Lamachour – 16, Pokhara, Nepal  
*bibash1270@gmail.com*

Tribhuvan University, Institute of Engineering, Pashchimanchal Campus,  
Department of Electronics and Computer Engineering, Lamachour – 16, Pokhara, Nepal  
*networkingamrit@gmail.com*

Tribhuvan University, Institute of Engineering, Pashchimanchal Campus,  
Department of Electronics and Computer Engineering, Lamachour – 16, Pokhara, Nepal  
*sunild@wrc.edu.np*

**Abstract:** This paper is an approach to predict the probability of an infected dermatoscopic image being cancerous (malignant melanoma) or not (benign) using learning power of Layered Convolutional Neural Network. Since the infected part of malignant highly resembles benign images, melanoma being the deadly fatal disease and confusion of dermatologists on differentiating malignant from benign easily has made this research a perfect application of machine learning to ease the field of Medical Science. Also, this research aims to propose computerized detection of malignant melanoma thereby preventing costly biopsy procedures that is otherwise done in clinic for diagnosing the disease. For this research, multiple architectures of layered neural network are designed, implemented and training is done by feeding those networks to around 13K dermatoscopic images using different training algorithms, multiple filters and tuning hyper-parameters in those algorithms to get the optimum result. 3 of the best performing milestone architectures with their hyper-parameter values and result analysis of those architectures is reflected in this paper. The best result we could achieve was with transfer learning using Google's Inception-v3 which resulted out the staggering 94.02% of training accuracy and 89.73% of validation accuracy with f1-score of 0.81.

**Keywords:** Computer Aided Detection and Diagnosis, Machine Learning, Neural nets, Pattern Recognition, Segmentation.

## 1. INTRODUCTION

Technology is increasing its range of invasion in the human world and medical field is no more an exception to it. Several advanced machines and system is being used to diagnosis the patients' diseases more easily and at early stage. Artificial Intelligence has also been used in the medical field in the past and present days to predict a person's proneness to disease, in image interpretation and recognition, in therapy planning and generating reminder's and alerts. Machine learning has been a boon to medical science because of its ability to diagnosis the disease fast and in accurate way, it's less chance of making errors, reduction in cost of treatment and encouraging the scope of telemedicine. Cancer is the unwanted growth of tissue in the human body. It can be fatal if not detected in its early stage and more importantly it starts revealing its symptoms in the later stage of the infection. Skin Cancer being one of the mostly occurring cancer, the number of people dying from this cancer has been increasing tremendously. Today's world, where the body of human have to spend most of their time of the day facing any sorts of radiation from modern highly equipped machines, the chance of people being prone to skin disease is also increasing. Skin Infection can be divided into two parts: Malignant and Benign. Malignant melanoma is one of the deadliest forms of cutaneous cancer, and one of the world's fastest growing cancers. Melanoma overall causes more deaths than any other type of skin cancer [1]. According to the American Cancer Society (ACS), in 2019 [2], it is estimated that there will be 96,480 new cases of melanoma in the United States and 7,230 deaths from the

disease. 57,220 cases of invasive melanoma will occur in males and 39,260 cases of invasive melanoma will occur in females [2]. The incidence of melanoma has been rising every year. Many of these lives could be saved if malignant melanoma were to be detected at the earliest stage, when it is easily curable [3]. Surveys reveal that there is a chance of 98% survival, if malignant is detected in early stage [4]. The main reason of its comparison with benign (non-cancerous) is because of its resemblance to benign infected images. The infected portions of skin inside the square boxes in Figure 1 too proves this fact. Dermatologic data shows that even in professional institutions, accuracy of visual diagnosis alone is not high. Hence, there are chances of confusion among the dermatologists in detecting whether the cancer is malignant or benign. And these confusions could easily contribute to more number of deaths in upcoming years too. Human life is precious one, and saving a single life also matters the most. Hence, trying to predict the type of cancer from the dermatoscopic images accurately by combining powerful merits of deep learning with neural network surely comes handy for dermatologists in the decision making process.

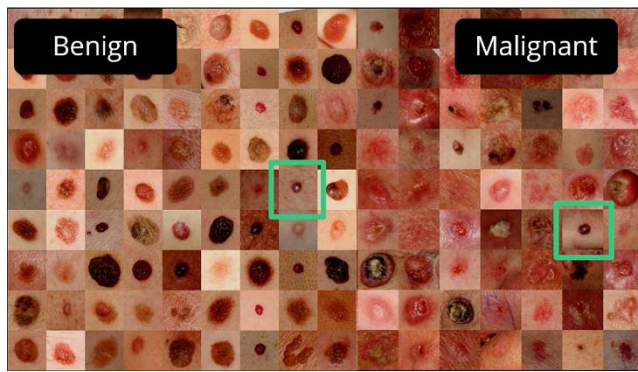


**Figure 1:** Benign and Malignant infected skin images. The sample in the squared box with one malignant and another benign shows they resemble each other.

## 2. LITERATURE REVIEW

### 2.1 Past Works

A number of studies using various technologies are being conducted around the world for the early detection of melanoma. In the field of medical imaging, in general, using neural networks for image segmentation is relatively rare. The existing traditional machine learning neural network algorithms still cannot completely solve the problem of information loss, nor detect the precise division of the boundary area. Previous literature referred to important techniques for early diagnosis of melanoma. Green *et al.* [5] proposed the use of shape, color and skin damage boundaries as features for technological classification. The system, consisting of a handheld device incorporating a color video camera and color frame grabber mounted in a microcomputer, was used in a pigmented lesion clinic. Analysis software extracted features relevant to the size, color, shape, and boundary of each lesion, and these features were correlated with clinical and histologic characteristics on which standard diagnoses of skin tumors are based. In a 10-month period, video images of 164 unselected pigmented lesions for which complete diagnostic data were available were successfully captured using the camera. Sixteen of 18 melanomas, and 89% of pigmented lesions overall, were correctly classified by the image analysis system. Masood *et al.* [6] proposed a standard automatic decision support system which is based on semantic analysis of melanoma images and further classification of characteristic objects commonly found in pigmented skin lesions. Preprocessing and segmentation of image was done and classification algorithms like k-Nearest Neighbor, Decision Trees, Logistic Regression, Artificial Neural Networks and Support Vector Machines and the review of all these comparative studies revealed that MLP gives better performance than Bayesian and kNN classifiers, while SVM with RBF kernel normally outperforms MLP, decision trees, and other statistical methods. Aitken *et al.* [7] classified the lesion area, perimeter, border, wavelength, and gradient. They captured video images of 5 lesions, all larger than 2 mm in greatest dimension, on each of 66 Australian adolescents on 2 occasions approximately 1 month apart. Features extracted by computer image analysis included area, perimeter, and regularity of outline of the lesions, the mean and standard deviation of reflectance at red, green, and blue wavelengths, and the mean and standard deviation of the gradients of red, green, and blue reflectance at the lesion boundary. All

measurements showed moderate to high reliability (intraclass correlation coefficients 0.66–0.94), except for the standard deviations of the color gradients, whose reliability improved to moderate levels (0.68–0.71) when the mean of 5 lesions was considered. For most outcomes, reasonable within subject reliability was achieved when five lesions per subject were measured. Chang *et al.* [8] proposed a heuristic method for feature extraction and lesion identification. A systematic heuristic approach is investigated for feature selection and lesion classification. The approach integrates statistical, correlation, histogram, and expert system based components. Using statistical and correlation measures, interrelationships among features are determined. Experimental results showed reduced lesion classification error rates based on condensing the shape and color feature set from 19 features to 13 features using the feature selection process. She *et al.* [9] classified melanoma skin lesions according to characteristics such as symmetry, border, color variation and diameter. Meanwhile, ABCD analysis was conducted to generate six features. They were asymmetry, border irregularity, colour (red, green and blue) variegations and diameter of lesion. The eight features of each case were combined using a principal component analysis (PCA) to produce two dominant features for lesion classification. A larger set of images containing malignant melanoma (MM) and benign naevi were processed as above and the scatter plot in a two dimensional dominant feature space showed excellent separation of benign and malignant lesions. An ROC (receiver operating characteristic) plot enclosed an area of 0.94. And Fassih *et al.* [10] used morphological operators and feature extraction via a wavelet transform technique to achieve melanoma segmentation. According to their paper, utilizing morphologic operators in segmenting and wavelet analysis in order to extract the features has culminated in better result in melanoma diagnosis. Their paper employs coefficients of wavelet decomposition to extract image's features. Melanoma classification is carried out by using the variance and mean of wavelet coefficients of images as the inputs of neural network. Results show 90% ability in distinction between benign and malignant lesions.

### 2.2 Our Approach to the Problem

The major similarity in above mentioned projects were the researchers themselves identified the features in the image and selected the features that could make impact upon the decision manually. Since, human eye is not capable of extracting small features, we allowed the machine to choose the feature by itself. Hence, rather than focusing on the specific parameter such as area of lesion, or perimeter, shape, wavelength, we fed the neural network the whole image and let it decide the features by itself because Convolutional Neural Network are believed to extract such features hidden from the human eye. Thus we have used an improved CNN layer to characterize and segment melanoma and benign images with multiple filters, activation functions and tuning of hyper-parameters for optimizing the loss algorithm.

## 3. METHODOLOGY

Our main objective is to construct a highly accurate classifier that generalizes well on data from new individuals. For this purpose, we tested the performance of different layered convolutional neural networks by switching between different optimization algorithms and tuning hyper-parameters, and assessed why some models performed well

while others performed poorly. Back Propagation Algorithm of machine learning is the major technique used along with multiple optimization algorithms, filter and parameter values. The process is highlighted in the flowchart presented in Figure 2.

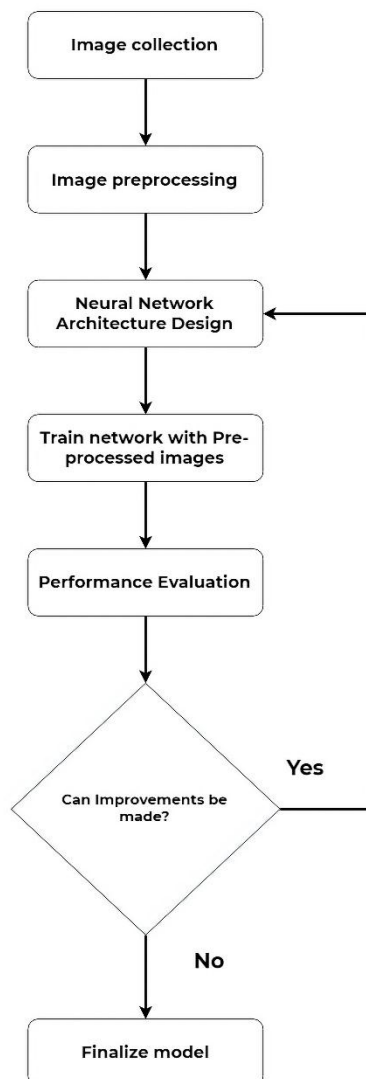


**Figure 2:** Flowchart presenting basic methodology of the research. Major 3 finalized model architecture is discussed in this paper along with its performance, its evaluation and analysis.

### 3.1 Datasets

The prime requirement for the project was the dermatoscopic images showing infected part caused by benign or malignant cancer. The courtesy of datasets is International Skin Image Collaboration (ISIC) [11] that consists of about 23K high resolution images of lesions which can be malignant (cancerous) or benign (non-cancerous).

### 3.2 Data Visualization and Pre-Processing

Once, we have downloaded 23K images, those images should be made ready to feed into the neural network. This is called image pre-processing. The data is too much skewed because, out of 23K data around 19K were benign and only 4K data were malignant. The main purpose in the analysis of pigmented skin lesion is to find out the difference in infected lesion and healthy skin. Detection of the lesion is a difficult problem in dermatoscopic images as the transition between

the lesion and the surrounding skin is smooth and even for trained dermatologist; it is a challenge to distinguish accurately [6]. It is seen that dermatoscopic images often contain components such as uneven illumination, dermatoscopic gel, black frames, ink markings, rulers, air bubbles, and intrinsic cutaneous features that can affect border detection such as blood vessels, hairs, and skin lines and texture [6]. Every such components that contribute to deformity in image and eventually affect the output of image processing and each of these factor should be considered for achieving robust lesion segmentation [12], [13]. Multiple approaches are used for identifying such regions and removing or masking them such as: image resizing, cropping part of image, masking, removing the hair (or attenuation) [14], [15] and conversion of image to intensity grey image [16], [17]. It helps to facilitate image segmentation through filtering and enhancing the important features of the lesion. Simple image translation, transformation, cropping the infected part and zooming infected portion are used [18]. Furthermore, most of the benign images are disturbed with medical instruments seen in the image, which might change the focus of neural networks while training. Hence, we manually removed such images which are thought to have less contribution to the improvement of the model and reduced the images to 13K out of which 3K images are malignant. Figure 3 shows the data distribution of images under each class.

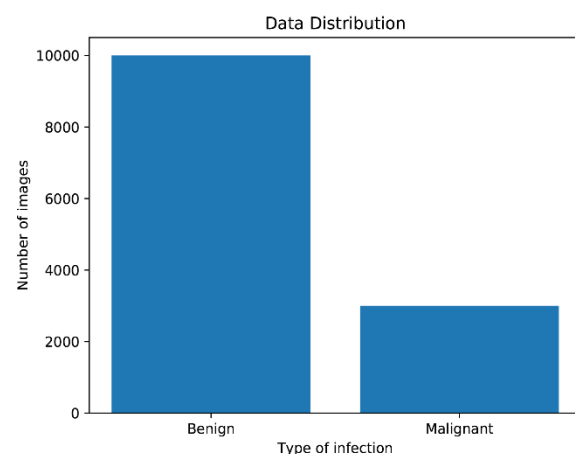


**Figure 3:** Final dataset distribution after the images are filtered. Out of 13K total images, 10K are benign and only 3K images are malignant.

### 3.3 Basic Algorithm

The problem is treated as binary classification problem where the two classes are Malignant and Benign and is represented by 1 and 0 respectively on the output of neural network. Each image is represented by  $m \times n \times 3$  matrix where each element represents the intensity of each pixel. Since all images are colored, third dimension of the matrix represents RGB values of each pixel. This data is the input to neural network and back propagation algorithm is used to adjust weights of each neuron. A neural network propagates the signal of the input data forward through its parameters towards the moment of decision, and then back-propagates information about the error, in reverse through the network, so that it can alter the parameters. Following steps occur while training a neural network:

- The network makes a guess about data, using its parameters.
- The network’s error is measured with a loss function.
- The error is back-propagated to adjust the wrong-headed parameters.

### 3.4 Neural Network Architecture

Different neural network architecture is sketched and implemented using the machine learning library and images are fed into the network. The network is trained with the training images and tested with unseen datasets to evaluate the ability of model to generalize across the problem domain. The major 3 models we found that was able to outstand other models are described below:

#### 3.4.1 1<sup>st</sup> Model

After having required number of datasets for this stage of project and formulated basic algorithm, simple neural network is used and data is fitted into the network to see how the network fares. It is mainly for preliminary viewing of the output result and carrying out the optimization as suggested by the output result. Simple Convolutional Neural Network is chosen having 3 convolution layers and two fully connected layer. The convolution layers were followed by Max-Pool operation. Rectified Linear Units (ReLU) are used as activation function for introducing non-linearity. Dropout is introduced for better learning. For optimization, multiple optimizer such as Adam Optimizer, Stochastic Gradient Descent is used with its default settings as the optimizer. Thus formed neural network architecture can be viewed in Figure 4.

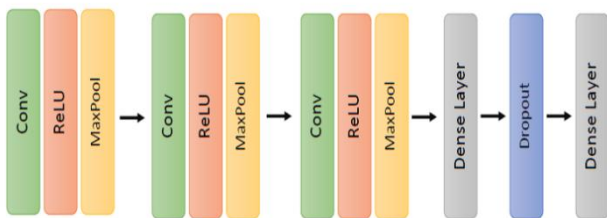


**Figure 4:** Architecture of Simple Convolutional Neural Network that was mainly for preliminary viewing of output result. The network contains 3 convolution layers each followed by Max-Pool operation and ReLU activation function and two fully connected layer at the end with proper dropout.

The total data is splitted into 80:20 (training set : testing set ratio). Images are scaled into 224\*224 pixels and batch size of 32 is set. The result output and performance analysis of this model is described in section 4.1.

#### 3.4.2 2<sup>nd</sup> Model

Upon analyzing the output from previous model, somehow deeper and denser network is used than that used in first model by increasing convolutional layers and fully connected layer, thus making it similar to VGGnet. Since, the deep network increases the chance of model being overfit, dropout is increased as a regularization parameter. The architecture of thus formed neural network can be viewed in Figure 5.

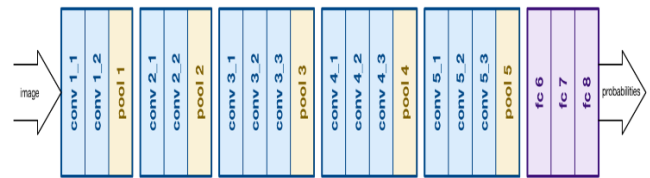


**Figure 5:** Architecture of further deeper and denser neural network developed after improving 1<sup>st</sup> model. Convolutional Layers has been increased followed by 3 fully connected layers, and thus making the network similar to VGGnet.

Data augmentation is introduced. Since, there is an imbalance in data, samples containing minority class is duplicated. Normal cropping, translation in the image is also done that could help in improvement of the model. The result output and performance analysis of this model is described in section 4.2.

#### 3.4.3 3<sup>rd</sup> Model

Since, the dataset was too much skewed and our previous network was failing to generalize for malignant images, we planned on using transfer learning. It is an approach in which a network already trained on large number of image is reused. We planned on using Inception-v3 model by Google. Trained inception model is loaded and it is used as a feature extractor. The output of the last convolution layer of the Inception model is extracted for all our images and is stored them offline. These outputs are called “bottlenecks” and are nothing but features of the images. Since the Inception model has been trained on the huge amount of data, it is able to extract relevant features like curves, edges, etc from the images which makes the extraction of features a lot easier. Once, the feature is extracted, a small network of 3 fully connected layers—2048\*512, 512\*512 and 512\*2 is created. This small network is then trained to classify the images into our two categories. An exponentially decaying learning rate is used and RMSProp, Adam and SGD’s are used as the optimizer. Since the inception model was used only as a feature extractor and not fine-tuned, our model became very simple. Thus, we were able to use a batch size of 128, which accelerated our training. Just like before, dropout ranging from 0.5 to 0.8 was used. Batch normalization is also tested. Neural network architecture can be viewed in Figure 6. The result output and performance analysis of this model is described in section 4.3.

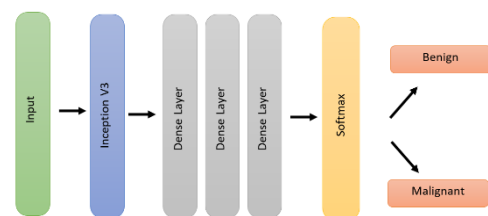


**Figure 6:** High Level overview of architecture of our neural network with Google’s Inception-v3 included inside it. The input image is fed into the 1<sup>st</sup> layer of Inception-v3. The final layer of inception-v3 is removed and 3 fully connected layers were added followed by a Softmax layer. In this way, we could be able to tune Inception-v3 according to our problem statement.

## 4. OUTPUT AND RESULT ANALYSIS

The output from the major 3 models that were built and trained upon are described and analyzed in this section.

### 4.1 Result from 1<sup>st</sup> Model

Using the architecture of the 1<sup>st</sup> model as described in Section 3.4.1, the data is trained using the training set and simultaneously the performance of network is tested using the testing set. The accuracy reported by this model is around 83.26 % achieved after 30 epochs and validation accuracy was 76.87%. On increasing epochs upto 60, accuracy increases to around 84.73 %. Accuracy and loss curves are shown in Figure 7. No significant increase in accuracy is seen. On running the model for many epochs (>150), training accuracy is found to be 97.74%, but the validation accuracy is just around 80.78%. This clearly showed that this model overfit the data. The optimum hyper-parameter values are: Learning Rate: 0.01, Activation Function: ReLU, Ratio of training to test: 80:20, Batch Size: 32, Optimization Algorithm: SGD with default settings, Image Size: 224\*224, Dropout: 0.9.

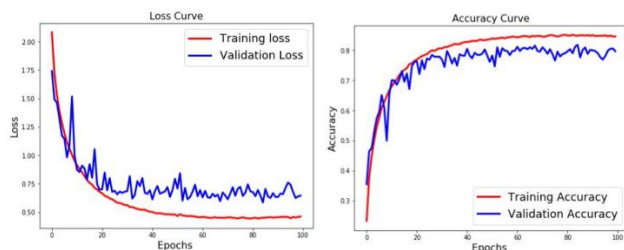


**Figure 7:** Accuracy and Loss curves on training 1<sup>st</sup> simple model of neural network. Upon training for more than 150 epochs, training accuracy went upto 97.74% while validation accuracy got saturated in 80.78% which concluded that the model overfit the data.

### 4.2 Result from 2<sup>nd</sup> Model

After not so expected performance from the 1st model, parameters are calibrated, several optimizers are tested and neural network is rebuilt as mentioned in Section 3.4.2 of this paper. Training through the new VGGnet look alike model, and playing around with the hyper-parameters, the maximum accuracy we could obtain was 89.21%. The accuracy curve is shown in Figure 8. The optimum hyper parameter values that got the best result are: Initial Learning Rate 0.1, Learning Rate Decay Factor: 0.01, Number of Steps per decay: 30, Activation Function: ReLU, Ratio of training set to testing set data: 80:20, Noise: 5, Batch Size: 32, Optimization Algorithm: Adam's optimizer with default settings, Dropout: 0.5, Image Size: 224\*224.

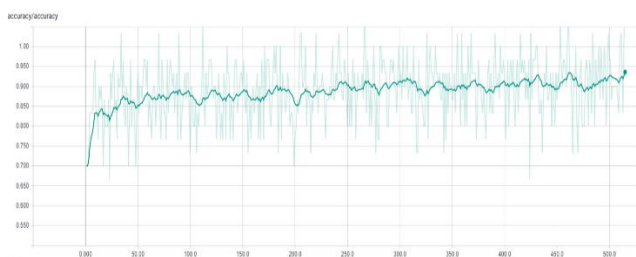


**Figure 8:** Accuracy curve after training data on 2<sup>nd</sup> Model of Neural Network. Improvements is seen comparing to 1<sup>st</sup> model, with less signs of overfit. But, upon training for more number of epochs also, the accuracy percentage got saturated to 89.21%.

With the skewed dataset, accuracy is not the best evaluation metric to decide the effectiveness of our neural network. Out of 13K total images, only 3K images are malignant. Thus, with a system that predicts every skin image as benign too will result in 81.25% accuracy. Hence, Precision, Recall and F1-Score provides the best view of the neural network result. Looking upon precision, recall and F1-Score calculated using 500 images of each malignant and benign, the result showed us that the model has somewhat equal calibre of recognizing minority class as it recognizes majority class.

Other evaluation metrics calculated from this model is shown in Table 1.

**Table 1:** Evaluation Metrics Calculated for 2<sup>nd</sup> Model

| Class     | Precision | Recall | F1 Score | Support |
|-----------|-----------|--------|----------|---------|
| Benign    | 0.73      | 0.77   | 0.75     | 500     |
| Malignant | 0.77      | 0.72   | 0.73     | 500     |
| Avg/Total | 0.75      | 0.74   | 0.74     | 1000    |

### 4.3 Result from 3<sup>rd</sup> Model

With no more significance improvement seen in the 2nd best model, we tried to rethink the learning process and came up with transfer learning as described in the Section 3.4.3. The Inception-v3 architecture was used and with the architecture described above, we were able to get an accuracy of 94.02% and validation accuracy was around 89.73 % which is an improvement of around 5% over our previous results. Hence, the transfer learning worked. The accuracy curve on training and validation set as well as cross entropy loss curve is shown in Figure 9 and Figure 10 respectively. The optimum hyper-parameter values are: Learning Rate: 0.1, Learning Rate Decay Factor: 0.16, Activation Function: ReLU, Ratio of Training to testing set: 80:20, Batch Size: 128, Optimization Algorithm: RMSProp, RMSProp Decay: 0.9, RMSProp Momentum: 0.9, RMSPropEpsilon: 1.0, Dropout: 0.75, Image Size: 299\*299.

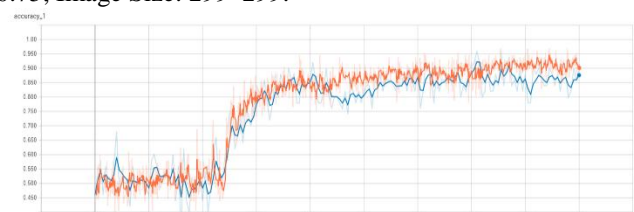


**Figure 9:** Accuracy curves generated while training our 3<sup>rd</sup> model on both training set and validation set. Since, it was transfer learning, low accuracy is reported for a while earlier which later got picked up rapidly. We could achieve training accuracy of 94.02% and testing accuracy of 89.73% hence, giving us the best result out of all models we tried on.

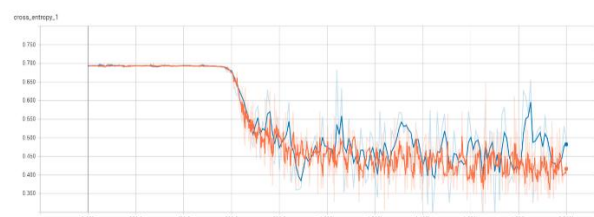


**Figure 10:** Cross Entropy Loss curve generated while training our 3rd model on both training set and validation set. The curve showed similar behavior as the accuracy curve, in a sense that it too stayed high for a while earlier, then, the loss went down rapidly in further epochs.

Other evaluation metrics calculated from this model is shown in Table 2.

**Table 2:** Evaluation Metrics Calculated for 3<sup>rd</sup> Model

| Class     | Precision | Recall | F1 Score | Support |
|-----------|-----------|--------|----------|---------|
| Benign    | 0.80      | 0.82   | 0.81     | 500     |
| Malignant | 0.82      | 0.80   | 0.81     | 500     |
| Avg/Total | 0.81      | 0.81   | 0.81     | 1000    |

Drastic improvement is seen upon calculating Precision, Recall and F1-Score of the model built using 3<sup>rd</sup> model of neural network, thanks to transfer learning.

#### 4.4 Analysis of Result

The output of the above models signified two major statements:

- The dataset we have used is not sufficient for the model to properly generalize.
- Raw neural networks which were not exposed to images previously, failed to properly learn more features of the image, but transfer learning outplayed every other architecture.

Because of the small dataset, the 1<sup>st</sup> and 2<sup>nd</sup> model didn't generalize enough to predict the image with higher accuracy. Especially, generalization is also poor due to the fact that malignant lesion image is of minor class. The dataset wasn't enough to properly teach network about feature extraction, boundary detection, etc. Also, the network was exposed to the image for the first time without any prior knowledge of image segmentation, boundary detection, etc. and with such small dataset it has to simultaneously learn basic image detection as well as generalize upon malignant and benign. While in case of 3<sup>rd</sup> model, since the architecture of Google's Inception – v3 was already trained on millions of image on the internet, it has already learnt to extract many features from the image. Utilizing this power to our dataset provided us an extra edge over previous two raw models. And, this resulted us an accuracy of staggering 94.02%. The comparison of parameters and output result of 3 prototypes that is built and tested upon in this paper is depicted in Table III.

**Table 3:** Comparison of Neural Network Architectures with Varying Parameters

| Parameters                 | Prototype 1 | Prototype 2 | Prototype 3 |
|----------------------------|-------------|-------------|-------------|
| Learning Rate (Initial)    | 0.01        | 0.1         | 0.1         |
| Learning Rate Decay Factor | -           | 0.01        | 0.16        |
| Activation Function        | ReLU        | ReLU        | ReLU        |
| Noise                      | -           | 5           | -           |
| Batch Size                 | 32          | 32          | 128         |

| Optimization Algorithm    | Stochastic Gradient Descent | Adam's Optimizer with Default Setting | RMSProp with Decay: 0.9 Momentum: 0.9 Epsilon: 1.0 |
|---------------------------|-----------------------------|---------------------------------------|--|
| Dropout                   | 0.9                         | 0.5                                   | 0.75   |
| Input Image Size          | 224*224                     | 224*224                               | 299*299  |
| Training Set: Testing Set | 80:20                       | 80:20                                 | 80:20  |
| Accuracy                  | 84.73%                      | 89.21%                                | 94.02%   |
| F1 Score (Avg)            | -                           | 0.74                                  | 0.81   |
| Recall (Avg)              | -                           | 0.75                                  | 0.81   |
| Precision (Avg)           | -                           | 0.74                                  | 0.81   |

## 5. CONCLUSION AND FUTURE ENHANCEMENTS

### 5.1 Conclusion

We have implemented the basics of deep learning using neural networks and also used transfer learning to detect to what extent is a skin image cancerous. We too have explored multiple layered convolutional neural network and trained the skin images with different hyper-parameters value and get the one with best evaluation metrics. Furthermore, we too tried different optimization algorithms to further improve the performance of model. And this resulted in the major 3 milestone architectures out of which Google's Inception – v3 stood apart from every other architecture with training accuracy of 94.02% and validation accuracy of 89.73% with f1-score of 0.81. Since, dermatoscopic images are so inexpensive to obtain and also are easily available, this encouraged us to apply image processing and machine learning algorithms by the help of which we are able to distinguish malignant melanoma from benign in this research paper.

### 5.2 Future Enhancements

We are further planning to improve the project for deployment. In machine learning, there is not a boundary that defines this model can't improve beyond this. There is always a room for improvement. Upon brainstorming, we are planning to extend this paper further addressing the following ideas to improve our model:

#### 5.2.1 Collecting more data

Since, the data is too skewed containing only 3K minority class image out of 13K total images, lack of enough dataset is the prime factor of our model performing below par.

#### 5.2.2 Increasing input features

The ISIC also provides age and sex information on the images in their metadata. Thus, those extra features could be used to see its impact on the model performance.

## DATA AVAILABILITY

The data used to support the findings of this study are available from the corresponding author upon request.

## CONFLICTS OF INTEREST

The authors declare that there are no conflicts of interest regarding the publication of this paper.

## ACKNOWLEDGEMENTS

The authors wish to Departmental Research Unit, Department of Electronics and Computer Engineering and Er. Hari Prasad Baral, Head of Department, Department of Electronics and Computer Engineering, Institute of Engineering, Pashchimanchal Campus, Nepal, for their continuous support and guidance throughout the journey of this paper.

## REFERENCES

- [1] M. Heath, N. Jaimes, B. Lemos, A. Mostaghimi, L. C. Wang, P. F. Peñas, and P. Nghiem, "Clinical characteristics of Merkel cell carcinoma at diagnosis in 195 patients: the AEIOU features," *Journal of the American Academy of Dermatology*, vol. 58, no 3, pp. 375-381, 2008.
- [2] American Cancer Society, "Facts & Figures 2019," American Cancer Society, Atlanta, Ga. 2019.
- [3] N. K. Mishra and M. E. Celebi, (2016, Jan). An Overview of Melanoma Detection in Dermoscopy Images using Image Processing and Machine Learning. [Online]. Available: <https://arxiv.org/ftp/arxiv/papers/1601/1601.07843.pdf>
- [4] The American Cancer Society medical and editorial content team, (2019, Feb). Survival Rates for Melanoma Skin Cancer. [Online]. Available: <https://www.cancer.org/cancer/melanoma-skin-cancer/detection-diagnosis-staging/survival-rates-for-melanoma-skin-cancer-by-stage.html>
- [5] A. Green, N. Martin, J. Pfitzner, M. O'Rourke, and N. Knight, "Computer Image Analysis in the Diagnosis of Melanoma," *Journal of the American Academy of Dermatology*, pp. 958-964, 1994.
- [6] A. Masood and A. A. Al-Jumaily, "Computer Aided Diagnostic Support System for Skin Cancer: A Review of Techniques and Algorithms," *International Journal of Biomedical Imaging*, Article Id: 323268, Jul, 2013.
- [7] J. F. Aitken, J. Pfitzner, D. Battistutta, P. K. O'Rourke, A. C. Green, and N. G. Martin, "Reliability of computer image analysis of pigmented skin lesions of Australian adolescents," *Cancer*, vol. 78, no 2, pp. 252-257, Jul, 1996.
- [8] Y. Chang, R. J. Stanley, R. H. Moss, and W. Van-Stoecker, "A systematic heuristic approach for feature selection for melanoma discrimination using clinical images," *Skin Research and Technology*, vol. 11, no 3, pp. 165-178, Aug, 2005.
- [9] Z. She, Y. Liu, and A. Damatoa, "Combination of features from skin pattern and ABCD analysis for lesion classification," *Skin Research and Technology*, vol. 13, no 1, pp. 25-33, Feb, 2007.
- [10] N. Fassihi, J. Shanbehzadeh, A. Sarafzadeh, E. Ghasemi, "Melanoma Diagnosis by the use of Wavelet Analysis based on Morphological Operators," in *Proc. IMECS*, Hong Kong, 2011.
- [11] International Skin Imaging Collaboration. ISIC Archive: The International Skin Imaging Collaboration: Melanoma Project. [Online]. Available: <https://isic-archive.com/>
- [12] M. E. Celebi, Q. Wen, H. Iyatomi, K. Shimizu, H. Zhon, and G. Schaefer, "A State-of-the-Art Survey on Lesion Border Detection in Dermoscopy Images," in *Dermoscopy Image Analysis*, M. E. Celebi, T. Mendonca, and J. S. Marques, Eds., Boca Raton, CRC Press, 2015, pp. 97-129.
- [13] F. Bogo, F. Peruch, A. B. Fortina and E. Peserico, "Where's the lesion? Variability in human and automated segmentation of dermoscopy images of melanocytic skin lesions," in *Dermoscopy Image Analysis*, M. E. Celebi, T. Mendonca and J. S. Marques, Eds., Boca Raton, CRC Press, 2015, pp. 67-96.
- [14] Q. Abbas, I. F. Garcia, M. E. Celebi, and W. Ahmad, "A Feature- Preserving Hair Removal Algorithm for Dermoscopy Images," *Skin Research and Technology*, vol. 19, no. 1, pp. 27-36, 2013.
- [15] Q. Abbas, M. E. Celebi, and I. F. García, "Hair removal methods: a comparative study for dermoscopy images," *Biomedical Signal Processing and Control*, vol. 6, no. 4, pp. 395-404, 2011.
- [16] R. Garnavi, M. Aldeen, M. E. Celebi, G. Varigos, and S. Finch, "Border detection in dermoscopy images using hybrid thresholding on optimized color channels," *Computerized Medical Imaging and Graphics*, vol. 35, no. 2, pp. 105-115, 2011.
- [17] G. Schaefer, M. I. Rajab, M. E. Celebi, and H. Iyatomi, "Colour and contrast enhancement for improved skin lesion segmentation," *Computerized Medical Imaging and Graphics*, vol. 35, no. 2, pp. 99-104, 2011.
- [18] R. J. Friedman, D. S. Rigel, and A. W. Kopf, "Early detection of malignant melanoma: The role of physician examination and self- examination of the skin," *CA: a cancer journal for clinicians*, vol. 35, no. 3, pp. 130-151, 1985.

## Author Profile



**Bishwa Raj Poudel** received the Bachelor's degree in Computer Engineering from the Tribhuvan University, Institute of Engineering, Pashchimanchal Campus, Pokhara, Nepal in 2019. Currently he is a Software Engineer at LIS Nepal Pvt. Ltd working on Online Stock Trading application named NOTS (Nepse Online Trading System). His research interests include problem solving using Machine Learning, designing multiple architectures of Neural Networks and analyzing the reason of under or over performance of each network.



**Bibash Adhikari** received the Bachelor's degree in Computer Engineering from the Tribhuvan University, Institute of Engineering, Pashchimanchal Campus, Pokhara, Nepal in 2019. Currently he is a Software Engineer at Utsaha Technologies working on building web applications and DevOps. His research interests include Deep Learning, Image Pre-processing techniques and Natural Language Processing.



**Amrit Koirala** received the Bachelor's degree in Computer Engineering from the Tribhuvan University, Institute of Engineering, Pashchimanchal Campus, Pokhara, Nepal in 2019. Currently he is System Administrator and Researcher in Networking Nepal working in different Networking and Cyber Security Projects. His research interests include Image Processing, Pattern Recognition, Networking Infrastructure Security and Cryptography.



**Sunil Dahal** received the Master's degree in Communication and Knowledge Engineering from the Tribhuvan University, Institute of Engineering, Pashchimanchal Campus, Pokhara, Nepal in 2018 and Bachelor's degree in Computer Engineering from Pokhara University in 2011. Currently he is Associate Campus Chief and a faculty member in Department of Electronics and Computer Engineering, Institute of Engineering, Pashchimanchal Campus, Tribhuvan University. His research interests include Deep Learning, Natural Language Processing and Image Processing.